



ELSEVIER

Nuclear Physics A 674 (2000) 527–538



www.elsevier.nl/locate/npe

Charge exchange in relativistic heavy-ion collisions

C.A. Bertulani¹, D.S. Dolci²

Instituto de Física, Universidade Federal do Rio de Janeiro, 21945-970 Rio de Janeiro, RJ, Brazil

Received 18 October 1999; revised 17 February 2000; accepted 6 March 2000

Abstract

Elastic charge-exchange in relativistic heavy ion collisions is responsible for the nondisruptive change of the charge state of the nuclei. We show that it can be reliably calculated within the eikonal approximation for the reaction part. The formalism is applied to the charge-pickup cross sections of 158 GeV/nucleon Pb projectiles on several targets. The relative contributions of pion- and rho-exchange are determined, using a single-particle model for the internal structure of the nuclei. The calculated cross sections are nonnegligible for heavy targets. It is shown that these cross sections can be useful to obtain information on the Gamow–Teller transition strengths of the nuclei. © 2000 Elsevier Science B.V. All rights reserved.

PACS: 25.70.Kk; 24.10.Ht

1. Introduction

Heavy-ion charge-pickup reactions can help us to access useful information on beta-decay transition strengths. At low energy nuclear collisions, it is well known that charge-exchange is accomplished by the proton exchange between the nuclei [1]. At intermediate energies (~ 100 MeV/nucleon) nucleon-exchange competes with the charged meson exchange [2]. At relativistic energies (> 1 GeV/nucleon), the charge stripping, $\Delta Z = -1$, cross sections will have a substantial contribution from proton removal [3], but the charge pickup, $\Delta Z = +1$, cross section will be solely due to the charged meson exchange, mainly π^\pm - and ρ^\pm -exchange [4]. It is virtually impossible that a proton-pickup will occur at these energies. The strong absorption of heavy ions selects large impact parameters and therefore emphasizes the longest range part of the charge exchange force. Since the reaction is very peripheral, one expects that the charge-exchange process is practically determined by the participation of the valence nucleons. Therefore, these reactions should

¹ bertu@if.ufrj.br

² dolci@if.ufrj.br

be a probe of charge exchange in a nuclear environment. A series of studies of this type has been performed theoretically and experimentally [5–8].

The charge-pickup cross sections for relativistic heavy ion collisions have recently been studied at CERN [9–12]. Theoretically, little is known about these reactions. It is the aim of this paper to develop a simple description of charge-pickup reactions in relativistic heavy ion collisions in terms of what we believe to be the most important ingredients, namely the microscopic π - and ρ -exchange potentials. An eikonal approach developed in Ref. [4] for charge-exchange in nucleus–nucleus scattering is used. Simple expressions are found which can be useful for estimation purposes in the planning of future experiments.

One basic assumption of our work is that the dominant process is pion and rho exchange between a projectile and a target nucleon. However, other mechanisms could also be of equal importance, i.e., $N + N \rightarrow N + \Delta$ followed by absorption. There has been a quite large number of measurements on spin–isospin excitations in charge-exchange ($^3\text{He}, t$) experiments at SATURNE that show the physics of these kind of processes are quite complicated. We will not study these questions in the present paper, leaving this for a future work. But, we refer to some of the SATURNE papers [13–16] for the interested reader.

In Section 2 we describe the reaction mechanism and the structure ingredients of our calculation. In Section 3 the dependence of the cross sections on the number of participants surface nucleons is studied in details and an application is done for the charge-pickup cross sections for 158 GeV/nucleon Pb projectiles on several targets. In Section 4 the proportionality of the measured cross sections to the Gamow–Teller strengths is shown. A comparison to the results of Section 3 shows that the reaction mechanism does not depend on the structure model. In Section 5 we present our conclusions.

2. Relativistic heavy-ion charge-exchange reactions

Following Ref. [4], the total cross section for charge-pickup cross sections in high energy heavy ion collisions is given by

$$\sigma = 2\pi \int_0^{\infty} b \mathcal{P}(b) db, \quad (2.1)$$

where \mathcal{P} is the probability of one-boson-exchange at the impact parameter b given by

$$\begin{aligned} \mathcal{P}(b) = & \left(\frac{1}{4\pi^2 \hbar v} \right)^2 (2j_P + 1)^{-1} (2j_T + 1)^{-1} \exp\{-2 \text{Im} \chi(b)\} \\ & \times \sum_{\nu, \mathbf{m}} |M(\mathbf{m}, \nu, b)|^2, \end{aligned} \quad (2.2)$$

where $\text{Im} \chi(b)$ is the imaginary part of the eikonal phase. In high energy collisions the phase $\chi(b)$ will be predominantly imaginary and can be constructed from the t -matrix for nucleon–nucleon scattering [17]. The matrix element $M(\mathbf{m}, \nu, b)$ carries information on the nuclear structure, and is given by

$$M(\mathbf{m}, \nu, b) = \int_0^\infty dq q J_\nu(qb) \int_0^{2\pi} d\phi_q e^{-i\nu\phi_q} \mathcal{M}(\mathbf{m}, \mathbf{q}) \quad (2.3)$$

with

$$\mathcal{M}(\mathbf{m}, \mathbf{q}) = \langle \Phi_f^P(\mathbf{r}_P) \Phi_f^T(\mathbf{r}_T) | e^{-i\mathbf{q}\cdot\mathbf{r}_P} V(\mathbf{q}) e^{i\mathbf{q}\cdot\mathbf{r}_T} | \Phi_i^P(\mathbf{r}_P) \Phi_i^T(\mathbf{r}_T) \rangle, \quad (2.4)$$

where $\Phi_{f(i)}^{P(T)}$ are the internal wavefunctions of the projectile (P) and target (T) in the initial (i) and final (f) states, respectively.

In Eq. (2.2), $\mathbf{m} = (m_T, m'_T, m_P, m'_P)$ is the set of angular momentum quantum numbers of the projectile and target wavefunction. \mathbf{m} is measured along the beam axis, and the subindices T and P refer to the target and projectile, respectively. The probability is obtained by an average of initial spins and a sum over final spins ($m_{P(T)}; m'_{P(T)}$). The interaction potential responsible for the charge-exchange between the nuclei is given by $V(\mathbf{q})$, where \mathbf{q} is the Fourier transform of the microscopic charge-exchange interaction. For more details, see [4].

Eqs. (2.1) and (2.2) are the basic results of the eikonal approach to the description of heavy-ion charge-exchange reactions at relativistic energies. They can also be used for the calculation of the excitation of Δ particles in nucleus–nucleus peripheral collisions. The essential quantity to proceed further is the matrix element given by Eq. (2.4) which is needed to calculate the impact-parameter-dependent amplitude $M(\mathbf{m}, \nu, b)$ through Eq. (2.3). The magnitude of this amplitude decreases with the decreasing overlap between the nuclei, i.e., with the impact parameter b . At small impact parameters the strong absorption will reduce the charge-exchange probability. Therefore, we expect that the probability given by Eq. (2.2) is peaked at the grazing impact parameter.

The pion + rho exchange potential, modified so that the zero range force is corrected for an extended source function [18], can be written as

$$V(\mathbf{q}) = V_\pi(\mathbf{q}) + V_\rho(\mathbf{q}) = [v(\mathbf{q})(\sigma_1 \cdot \hat{\mathbf{q}})(\sigma_2 \cdot \hat{\mathbf{q}}) + w(\mathbf{q})(\sigma_1 \cdot \sigma_2)] (\tau_1 \cdot \tau_2), \quad (2.5)$$

where

$$v(\mathbf{q}) = v_\pi^{\text{tens}}(\mathbf{q}) + v_\rho^{\text{tens}}(\mathbf{q}), \quad \text{and} \quad (2.6)$$

$$w(\mathbf{q}) = w_\pi^{\text{cent}}(\mathbf{q}) + \xi w_\rho^{\text{cent}}(\mathbf{q}) + w_\pi^{\text{tens}}(\mathbf{q}) + w_\rho^{\text{tens}}(\mathbf{q}),$$

and

$$v_\pi^{\text{tens}}(\mathbf{q}) = -J_\pi \frac{\mathbf{q}^2}{m_\pi^2 + \mathbf{q}^2}, \quad v_\rho^{\text{tens}}(\mathbf{q}) = J_\rho \frac{\mathbf{q}^2}{m_\rho^2 + \mathbf{q}^2}, \quad (2.7)$$

$$w_\pi^{\text{cent}}(\mathbf{q}) = -\frac{1}{3} J_\pi \left[\frac{\mathbf{q}^2}{m_\pi^2 + \mathbf{q}^2} - 3 g'_\pi \right], \quad (2.8)$$

$$w_\rho^{\text{cent}}(\mathbf{q}) = -\frac{2}{3} J_\rho \left[\frac{\mathbf{q}^2}{m_\rho^2 + \mathbf{q}^2} - \frac{3}{2} g'_\rho \right],$$

$$w_\pi^{\text{tens}}(\mathbf{q}) = \frac{1}{3} J_\pi \frac{\mathbf{q}^2}{m_\pi^2 + \mathbf{q}^2}, \quad w_\rho^{\text{tens}}(\mathbf{q}) = -\frac{1}{3} J_\rho \frac{\mathbf{q}^2}{m_\rho^2 + \mathbf{q}^2} \quad (2.9)$$

with the parameters $g'_\pi = 1/3$, $g'_\rho = 2/3$, and $\xi = 0.4$ [19].

The values of the coupling constants J_π and J_ρ in nuclear units are given by

$$\begin{aligned} J_\pi &= \frac{f_\pi^2}{m_\pi^2} \equiv f_\pi^2 \frac{(\hbar c)^3}{(m_\pi c^2)^2} \simeq 400 \text{ MeV fm}^3, \\ J_\rho &= \frac{f_\rho^2}{m_\rho^2} \equiv f_\rho^2 \frac{(\hbar c)^3}{(m_\rho c^2)^2} \simeq 790 \text{ MeV fm}^3, \end{aligned} \quad (2.10)$$

where $f_\pi^2/4\pi = 0.08$ ($f_\rho^2/4\pi = 4.85$), $m_\pi c^2 = 145 \text{ MeV}$ and $m_\rho c^2 = 770 \text{ MeV}$.

Turning off the terms $w_{\pi,\rho}^{\text{cent}}$, or $v_{\pi,\rho}^{\text{tens}}$ and $w_{\pi,\rho}^{\text{tens}}$ allows us to study the contributions from the central and the tensor interaction, and from π - and ρ -exchange, respectively.

Using Eq. (2.5), and single-particle wavefunctions, $\phi_{j\ell m}$, it is straightforward to show that Eq. (2.4) reduces to [4] (note that here the indexes π and ν denote the proton and the neutron wavefunctions, respectively):

$$\begin{aligned} \mathcal{M}(\mathbf{m}, \mathbf{q}) &= w(\mathbf{q}) \sum_{\mu} \langle \phi_{j'_T \ell'_T m'_T}^{(\pi)} | \sigma_{\mu} e^{i\mathbf{q}\cdot\mathbf{r}} | \phi_{j_T \ell_T m_T}^{(\nu)} \rangle \langle \phi_{j'_P \ell'_P m'_P}^{(\nu)} | \sigma_{\mu} e^{-i\mathbf{q}\cdot\mathbf{r}} | \phi_{j_P \ell_P m_P}^{(\pi)} \rangle \\ &\quad + \frac{4\pi}{3} v(\mathbf{q}) \sum_{\mu\mu'} Y_{1\mu}(\hat{\mathbf{q}}) Y_{1\mu'}(\hat{\mathbf{q}}) \langle \phi_{j'_T \ell'_T m'_T}^{(\pi)} | \sigma_{\mu} e^{i\mathbf{q}\cdot\mathbf{r}} | \phi_{j_T \ell_T m_T}^{(\nu)} \rangle \\ &\quad \times \langle \phi_{j'_P \ell'_P m'_P}^{(\nu)} | \sigma_{\mu'} e^{-i\mathbf{q}\cdot\mathbf{r}} | \phi_{j_P \ell_P m_P}^{(\pi)} \rangle. \end{aligned} \quad (2.11)$$

Expanding $e^{i\mathbf{q}\cdot\mathbf{r}}$ into multipoles we can write:

$$\langle \phi_{j'_\ell m'}^{(\pi)} | \sigma_{\mu} e^{i\mathbf{q}\cdot\mathbf{r}} | \phi_{j\ell m}^{(\nu)} \rangle = 4\pi \sum_{IM} i^I Y_{IM}^*(\hat{\mathbf{q}}) \langle \phi_{j'_\ell m'}^{(\pi)} | j_I(qr) Y_{IM}(\hat{\mathbf{r}}) \sigma_{\mu} | \phi_{j\ell m}^{(\nu)} \rangle. \quad (2.12)$$

Since $j_I(qr) Y_{IM}(\hat{\mathbf{r}})$ is an irreducible tensor,

$$\sigma_{\mu} j_I(qr) Y_{IM}(\hat{\mathbf{r}}) = \sum_{I'M'} (I1M\mu|I'M') \Psi_{I'M'}, \quad (2.13)$$

where $\Psi_{I'M'}$ is also an irreducible tensor. Therefore,

$$\begin{aligned} &\langle \phi_{j'_\ell m'}^{(\pi)} | \sigma_{\mu} j_I(qr) Y_{IM}(\hat{\mathbf{r}}) | \phi_{j\ell m}^{(\nu)} \rangle \\ &= \sum_{I'M'} (I1M\mu|I'M') \langle \phi_{j'_\ell m'}^{(\pi)} | \Psi_{I'M'} | \phi_{j\ell m}^{(\nu)} \rangle \\ &= \sum_{I'M'} (I1M\mu|I'M') (j'I'mM'|j'm') \langle \phi_{j'}^{(\pi)} || \Psi_{I'} || \phi_j^{(\nu)} \rangle. \end{aligned} \quad (2.14)$$

Eqs. (2.11)–(2.14) allows one to calculate the charge-exchange between single-particle orbitals. The quantity needed is the reduced matrix element $\langle \phi_{j'}^{(\pi)} || [j_I(qr) \sigma \otimes Y_I]_{I'} || \phi_j^{(\nu)} \rangle$. These are calculated in textbooks of nuclear structure (see, e.g., [20]). If several orbitals contribute to the process, the respective amplitudes can be added and further on averaged in the cross sections.

3. Single-particle matrix-elements and surface approximation

The reduced matrix elements are calculated in the single-particle model for neutrons and protons. Using Eq. (A.2.24) of Ref. [20] one finds:

$$\begin{aligned}
 & \langle \phi_{j'}^{(\pi)} \parallel [j_I(qr) \sigma \otimes Y_I]_{I'} \parallel \phi_j^{(v)} \rangle \\
 &= -(-1)^{\ell+\ell'+j'-1/2} \left\{ \frac{2j+1}{4\pi(2I'+1)} \right\}^{1/2} \left(jj' \frac{1}{2} - \frac{1}{2} \middle| I' 0 \right) \\
 & \times \left\{ \frac{1+(-1)^{\ell+\ell'+I}}{2} \right\} \begin{pmatrix} \sqrt{I+1} & 1/\sqrt{I+1} \\ 0 & \sqrt{\{(2I+1)/I(I+1)\}} \\ -\sqrt{I} & 1/\sqrt{I} \end{pmatrix} \\
 & \times \left(\frac{1}{(-1)^{\ell+1/2-j} \eta_{I'}(jj')} \right) \mathcal{F}_{Ijj'}(q), \tag{3.1}
 \end{aligned}$$

where

$$\mathcal{F}_{Ijj'}(q) = \int_0^\infty R_j^{(\pi)}(r) R_{j'}^{(v)}(r) j_I(qr) r^2 dr \quad \text{and} \tag{3.2}$$

$$\eta_{I'}(jj') = \frac{1}{2} \{ (2j+1) + (-1)^{j+j'-I'} (2j'+1) \}. \tag{3.3}$$

In Eq. (3.2), $R_j^{(\pi)}(r)$ and $R_{j'}^{(v)}(r)$ are the proton and neutron single-particle radial wavefunctions, respectively.

The (3×2) and (2×1) arrays in the equation are matrices and matrix multiplication is implied. The resulting matrix A_{mn} is a (3×1) array with A_{11} , A_{21} and A_{31} the values of the reduced matrix elements when $I' = I + 1$, I , and $I - 1$, respectively. The factor $[1 + (-1)^{\ell+\ell'+I}]/2$ vanishes unless $\ell + \ell' + I$ is even, that is unless parity is conserved.

The proton and neutron wavefunctions which are needed for the integral Eq. (3.2) must carefully account for the Pauli blocking in the final state. Moreover, the pion, or ρ , is readily absorbed in the nuclear surface and only the nucleons in the last shells and close to the nuclear surface will contribute to the process. The surface approximation consists in using

$$4\pi \langle R_j^{(\pi)}(r) R_{j'}^{(v)}(r) \rangle = N_s \rho(r), \tag{3.4}$$

where $\langle \rangle$ means the average over the N_s participant surface nucleons, and is $\rho(r)$ the nuclear density. To simplify, we also use $\ell = \ell' = 0$, so that only the spin of the nucleons are considered in the following developments. This will limit $I' = 1$, and $I = 0$. Thus, the relevant matrix element is

$$\langle \phi_{1/2}^{(\pi)} \parallel [j_0(qr) \sigma \otimes Y_0]_1 \parallel \phi_{1/2}^{(v)} \rangle = -\frac{1}{2} \sqrt{\frac{3}{\pi}} \mathcal{F}_0(q). \tag{3.5}$$

The Woods–Saxon distribution with central density ρ_0 , radius R_0 and diffusiveness a gives a good description of the densities of the nuclei involved in our calculation. However,

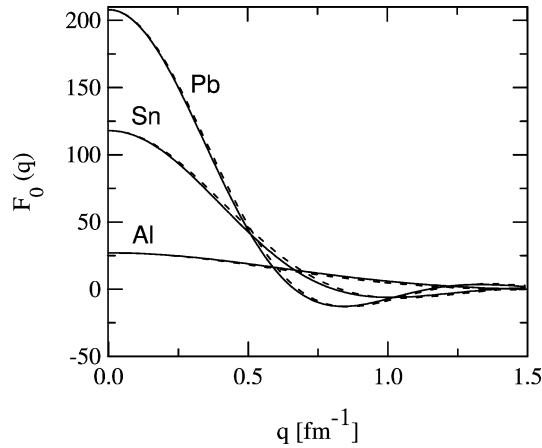


Fig. 1. The form factor $\mathcal{F}_0(q)$ of Eq. (3.6), compared to the one obtained by the numerical integration using Woods–Saxon density distributions for Al, Cu, Sn, Au, and Pb (to simplify the figure, we did not plot the curves for Au and Cu).

this distribution is very well described by the convolution of a hard sphere and an Yukawa function [23]. In this case, $\mathcal{F}_0(q)$ can be calculated analytically [21]:

$$\mathcal{F}_0(q) = \frac{4\pi\rho_0}{q^3} [\sin(qR_0) - qR_0 \cos(qR_0)] \left[\frac{1}{1 + q^2 a_Y^2} \right]. \quad (3.6)$$

Fig. 1 compares $\mathcal{F}_0(q)$ obtained with the numerical integration with the Woods–Saxon density distribution for Al ($R_0 = 3.07$ fm, $a = 0.519$ fm), Cu ($R_0 = 4.163$ fm, $a = 0.606$ fm), Sn ($R_0 = 5.412$ fm, $a = 0.560$ fm), Au ($R_0 = 6.43$ fm, $a = 0.541$ fm) and Pb ($R_0 = 6.62$ fm, $a = 0.546$ fm) (to simplify the figure, we did not plot the curves for Au and Cu). In all cases we used the Yukawa function parameter in Eq. (3.6) $a_Y = 0.7$ fm. We see that the agreement is very good. For carbon, one can use a Gaussian density, with the Gaussian parameter $a = \sqrt{\frac{2}{3}}(r^2)_C = 2.018$ fm². In this case,

$$\mathcal{F}_0(q) = \pi^{3/2} \rho_0 a^{5/2} \exp(-q^2 a^2 / 4). \quad (3.7)$$

A further simplification can be obtained for the factor $T(b) = \exp(-2 \text{Im} \chi(b))$ in Eq. (2.2). We use the “ $t\rho\rho$ ” approximation [17], which gives

$$T(b) = \exp \left\{ -\sigma_{NN} \int_{-\infty}^{\infty} dz \int \rho_P(\mathbf{r}) \rho_T(\mathbf{R} + \mathbf{r}) d^3 r \right\} \quad (3.8)$$

with $\mathbf{R} = (\mathbf{b}, z)$. σ_{NN} is the nucleon–nucleon cross section at the corresponding bombarding energy, and $\rho_{P(T)}$ is the projectile (target) matter density distribution. $T(b)$ is known as the transparency function. At 158 GeV/nucleon we use $\sigma_{NN} = 52$ mb.

The simplest parameterization for the nuclear matter densities are Gaussian functions. Assuming

$$\rho_{P(T)}(r) = \rho_{P(T)}(0) \exp\{-r^2 / \alpha_{P(T)}^2\}, \quad (3.9)$$

the integrals in Eq. (3.8) can be performed analytically. One gets:

$$T(b) = \exp\left\{-\frac{\pi^2 \sigma_{NN} \rho_T(0) \rho_P(0) \alpha_T^3 \alpha_P^3}{(\alpha_T^2 + \alpha_P^2)} \exp\left[-\frac{b^2}{(\alpha_T^2 + \alpha_P^2)}\right]\right\}. \quad (3.10)$$

As observed by Karol [22], for nuclei which densities well described by Woods–Saxon distributions, $T(b)$ is very little dependent on the lower values of b and consequently on the values of $\rho_{P(T)}(r)$ for small r 's. Only the surface form of the density is relevant. Thus one can fit the surface part of the densities by Gaussian functions and use the Eq. (3.10) with the appropriate fitting parameters $\rho_P(0)$, $\rho_T(0)$, a_T and a_P . If the density distributions is given by a Fermi or Woods–Saxon function

$$\rho(r) = \rho_0 \{1 + \exp[(r - R)/(t/4.4)]\}^{-1}. \quad (3.11)$$

Karol [22] has shown that $T(b)$ can be well reproduced with Gaussian fits for the nuclear densities, if the parameters in the Gaussian distributions (3.9) are given by

$$\alpha^2 = \frac{4Rt + t^2}{k}, \quad \rho(0) = \frac{1}{2} \rho_0 e^{R^2/\alpha^2}, \quad (3.12)$$

where

$$\rho_0 = \frac{3A}{4\pi R^3 [1 + (\pi^2 t^2/19.36R^2)]}, \quad k = 4(\ln 5) = 6.43775 \dots, \quad (3.13)$$

and A is the mass number.

In Fig. 2 we compare the Karol transparency functions (open circles) with the ones obtained by a numerical integration of the integral (3.8) with Woods–Saxon densities (solid

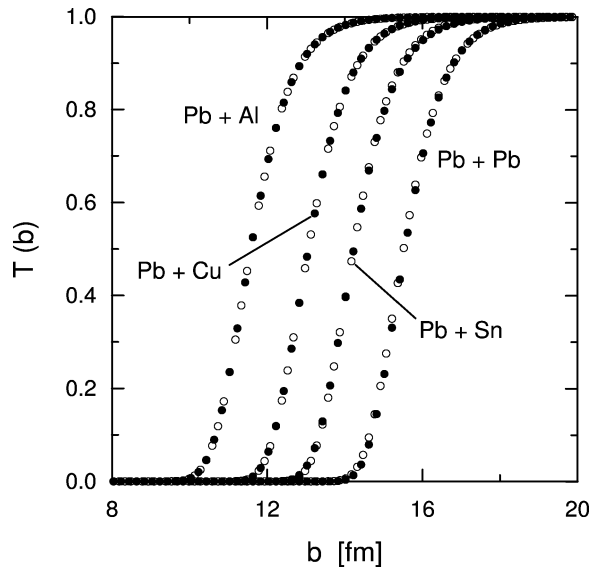


Fig. 2. Comparison of the Karol transparency functions (open circles) with the ones obtained by a numerical integration of the integral (3.8) with Woods–Saxon densities (solid circles).

circles). The agreement is excellent. Thus, the calculation simplifies enormously with the use of this approximation.

In Eq. (2.4), only the transverse part of \mathbf{q} is needed. Using

$$Y_{\ell m}(\hat{\mathbf{q}}_t) = \begin{cases} (-1)^{(\ell+m)/2} \left(\frac{2\ell+1}{4\pi}\right)^{1/2} \frac{[(\ell-m)!(\ell+m)!]^{1/2}}{(\ell-m)!(\ell+m)!} e^{im\phi}, & \text{if } \ell + m = \text{even,} \\ 0, & \text{otherwise,} \end{cases} \quad (3.14)$$

and

$$\int_0^{2\pi} e^{i(m-\nu)\phi} d\phi = 2\pi \delta_{m,\nu} \quad (3.15)$$

in the matrix elements (2.11)–(2.14), it is straightforward to show that (2.3) becomes

$$M(\mathbf{m}, \nu, b) = C_0(m_P, m'_P, m_T, m'_T) F_0(b) + C_\nu(m_P, m'_P, m_T, m'_T) G_\nu(b),$$

where

$$C_0(m_P, m'_P, m_T, m'_T) = \frac{3}{2} \sum_{\mu} \left(\frac{1}{2} 1 m_P \mu \middle| \frac{1}{2} m'_P\right) \left(\frac{1}{2} 1 m_T \mu \middle| \frac{1}{2} m'_T\right),$$

$$C_\nu(m_P, m'_P, m_T, m'_T) = \frac{3}{4} \sum_{\mu\mu'} \left(\frac{1}{2} 1 m_P \mu \middle| \frac{1}{2} m'_P\right) \left(\frac{1}{2} 1 m_T \mu' \middle| \frac{1}{2} m'_T\right) \delta_{\mu-\mu',\nu} \quad (3.16)$$

and

$$F_0(b) = \int_0^\infty dq q J_0(qb) w(q) \mathcal{F}_0^2(q), \quad G_\nu(b) = \int_0^\infty dq q J_\nu(qb) v(q) \mathcal{F}_0^2(q). \quad (3.17)$$

In Fig. 3 we plot the charge-pickup probabilities for Pb (158 GeV/nucleon) + X (target), with X = C, Al, Cu, Sn, Au and Pb. The exchange probability is peaked at grazing impact parameters: at low impact parameters the strong absorption makes the probability small, whereas at large impact parameters it is small because of the short-range of the exchange potentials. The value of the exchange probability at the peak is about 10^{-5} for Pb + Pb. As

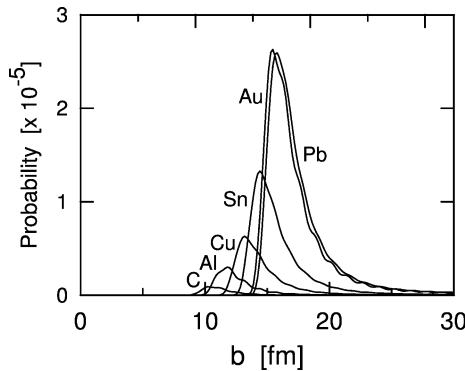


Fig. 3. Charge-pickup probabilities for Pb (158 GeV/nucleon) + X (target), with X = C, Al, Cu, Sn, Au and Pb.

in the case studied in Ref. [4] the process is dominated by π -exchange, with only a small fraction, of the order of 10%, or less, originating from the ρ exchange channel.

The probabilities are divided by the square of the number of participating nucleons. As shown, it increases with the target mass number. The cross sections are found out to be approximately constant for bombarding energies above 10 GeV/nucleon. The reason is simple, since from Eq. (2.2) we see that, apart from the factor $(1/v)^2 \sim (1/c)^2$, the only energy dependence comes from the total nucleon–nucleon cross section in the absorption factor $T(b)$. This is approximately constant at relativistic energies.

In Fig. 4 we plot the total charge-pickup cross sections in Pb (158 GeV/nucleon) + X (target), with X = C, Al, Cu, Sn, Au and Pb. The dashed line is a guide to the eyes. The solid line is explained in next section. The cross section is also divided by the square of the number of participating nucleons. It increases steadily with the target mass number.

In Table 1 we give the values of σ/N_s^2 (in mb) for the studied reactions.

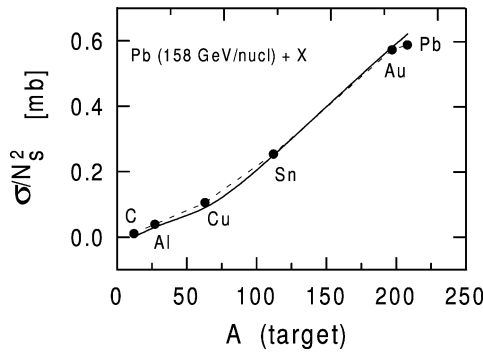


Fig. 4. Total charge-pickup cross sections for Pb (158 GeV/nucleon) + X (target), with X = C, Al, Cu, Sn, Au and Pb. The dashed curve is a guide to the eyes. The solid curve represents a calculation of the cross sections divided by the Gamow–Teller transition strengths of the nuclei and normalized to the σ/N_s^2 cross section for Pb + Sn.

Table 1

Total charge-pickup cross sections (per participant nucleon) for Pb (158 GeV/nucleon) + X (target), with X = C, Al, Cu, Sn, Au and Pb

Pb (158 GeV/nuc) + X	σ/N_s^2 (mb)
C	0.0106
Al	0.0394
Cu	0.105
Sn	0.253
Au	0.572
Pb	0.587

4. Proportionality to the Gamow–Teller transition strengths

It is clear that the approximation (3.4) is very rough and that the assumption of $\ell = 0$ nucleons at the surface is not realistic, specially because the surface nucleons are certainly not in an s -wave state. However, these approximations have been useful to extract the main features of the reaction mechanism in relativistic $\pi + \rho$ exchange. Some of these features are very useful for further theoretical developments. It is clear from Figs. 2 and 3 that only nucleons very close to the surface will contribute to the process. Thus, one can simplify these approximations by replacing the nucleon coordinates in Eq. (2.11) by their surface positions, \mathbf{R}_P and \mathbf{R}_T , respectively. In this case Eq. (2.11) reduces to the very compact expression

$$\mathcal{M} = [w(q) + v(q)] M_{\text{GT}}(P \rightarrow P') M_{\text{GT}}(T \rightarrow T') e^{i\mathbf{q}\cdot\mathbf{R}_P} e^{i\mathbf{q}\cdot\mathbf{R}_T}, \quad (4.1)$$

where we also used Eq. (3.14). The Gamow–Teller matrix elements M_{GT} are expectation values of the $\sigma\tau$ operators, i.e.,

$$M_{\text{GT}}(A \rightarrow A') = \int d^3r \rho_{\sigma\tau}(\mathbf{r}) = \langle A' | \sigma\tau | A \rangle. \quad (4.2)$$

Inserting Eq. (4.1) into Eqs. (2.4) and (2.2), and using the integral

$$\int d\phi \exp(-i\nu\phi) \exp(-iqx \cos\phi) = 2\pi J_\nu(qx), \quad (4.3)$$

we get:

$$\begin{aligned} \mathcal{P}(b) &= \left(\frac{1}{4\pi^2 \hbar\nu} \right)^2 \exp\{-2\text{Im}\chi(b)\} B_{\text{GT}}(P \rightarrow P') B_{\text{GT}}(T \rightarrow T') \\ &\quad \times \sum_\nu |H(\nu, b)|^2, \end{aligned} \quad (4.4)$$

where

$$B_{\text{GT}}(A \rightarrow A') = |M_{\text{GT}}(A \rightarrow A')|^2 = |\langle A' | \sigma\tau | A \rangle|^2 \quad (4.5)$$

is the Gamow–Teller transition strength of nucleus A . A sum over final spins and average over initial spins is implicit. The function $H(\nu, b)$ is given by

$$H(\nu, b) = 2\pi \int_0^\infty dq q [w(q) + v(q)] J_\nu(qb) J_\nu[q(R_P + R_T)]. \quad (4.6)$$

This function is peaked at $b = R_P + R_T$ and its width is determined by the range of the pion-exchange interaction, i.e., $\Delta b \sim 1$ fm.

The expression (4.4) shows the proportionality between the charge exchange probabilities and the Gamow–Teller transition strengths in relativistic heavy-ion collisions. A similar relationship was obtained by Taddeucci et al. [24] for (p, n) reactions at 0 degrees for proton energies of ~ 100 MeV. For heavy-ion reactions at 0 degrees and bombarding energies of ~ 100 MeV, a similar relationship was also obtained by Osterfeld et al. [25]. The validity of such a proportionality depends on the factorization of the cross sections into

two terms, one depending on the nuclear sizes and absorption, and the other on the nuclear structure. The solid line in Fig. 4 displays the cross sections for charge-pickup reactions using the proportionality expression (4.4). The results have been normalized to yield the same magnitude as σ/N_s^2 for the reaction Pb (158 GeV/nucleon) + Sn. One sees that the agreement is excellent, showing that the A -dependence of the process is solely due to geometry factors (nuclear transparency and the range of the one-boson-exchange interaction). The oversimplified model of the last section is thus unnecessary, but it was useful to show that one can use the proportionality expression (4.4) to access precious information on the beta-decay strengths from charge-pickup reactions with relativistic heavy ions.

5. Conclusions

We described the charge exchange in relativistic heavy ion reactions in terms of π and ρ exchange and the eikonal approximation. We applied the formalism to the calculation of charge-pickup probabilities and cross sections for Pb (158 GeV/nucleon) + X (target), with X = C, Al, Cu, Sn, Au and Pb.

Our model yields probabilities and cross sections which are dependent on the number of participating nucleons at the nuclear surface. The cross sections for the process are not small, as seen from Fig. 4. Assuming, e.g., that the number of surface nucleons which can contribute to the process is of order of 10 for large systems, one gets cross sections of order of 50 mb, or more.

The calculation is useful to support the proportionality of the measured cross sections with the Gamow–Teller matrix transition strengths. These are useful nuclear structure information. However, the experiments would have to be able to distinguish these “elastic” charge-exchange events from more complicated backgrounds, e.g., charge-exchange with pion production.

Acknowledgements

The authors have benefited from many suggestions and fruitful discussions with C. Scheidenberger and K. Suemmerer.

This work was partially supported by the Brazilian funding agencies FAPERJ, CNPq, FUJB/UFRJ, and by MCT/FINEP/CNPQ(PRONEX) under contract No. 41.96.0886.00.

References

- [1] H. Feshbach, *Theoretical Nuclear Physics: Nuclear Reactions*, Wiley, New York, 1992.
- [2] H. Lenske, H.H. Wolter, H.G. Bohlen, *Phys. Rev. Lett.* 62 (1989) 1457.
- [3] B.V. Carlson, R. Mastroleo, M.S. Hussein, *Phys. Rev. C* 46 (1992) R30.
- [4] C.A. Bertulani, *Nucl. Phys. A* 554 (1993) 493.
- [5] E. Oset, E. Shiino, H. Toki, *Phys. Lett. B* 224 (1989) 249.
- [6] T. Udagawa, P. Oltmanns, F. Osterfeld, S.W. Hong, *Phys. Rev. C* 49 (1994) 3162.

- [7] B. Ramstein et al., *Eur. Phys. J. A* 6 (1999) 225.
- [8] K. Sneppen, C. Gaarde, *Phys. Rev. C* 50 (1994) 338.
- [9] S.E. Hirzebruch et al., *Phys. Rev. C* 51 (1995) 2085.
- [10] S. Geer et al., *Phys. Rev. C* 52 (1995) 334.
- [11] H. Dekhissi et al., CERN/Preprint DFUB 98-19.
- [12] C. Scheidenberger, private communication.
- [13] C. Ellgaard et al., *Phys. Rev. Lett.* 50 (1983) 1745.
- [14] C. Ellgaard et al., *Phys. Lett. B* 154 (1985) 110.
- [15] D. Contardo et al., *Phys. Lett. B* 168 (1986) 331.
- [16] I. Bergqvist et al., *Nucl. Phys. A* 469 (1987) 648.
- [17] M.S. Hussein, R. Rego, C.A. Bertulani, *Phys. Rep.* 201 (1991) 279.
- [18] G.F. Bertsch, H. Esbensen, *Rep. Prog. Phys.* 50 (1987) 607.
- [19] M.R. Anastasio, G.E. Brown, *Nucl. Phys. A* 285 (1977) 516.
- [20] R.D. Lawson, *Theory of the Nuclear Shell Model*, Clarendon Press, Oxford, 1980.
- [21] S. Klein, J. Nystrand, *Phys. Rev. C* 60 (1999) 014903.
- [22] P.J. Karol, *Phys. Rev. C* 11 (1975) 1203.
- [23] K.T.R. Davies, J.R. Nix, *Phys. Rev. C* 14 (1976) 1977.
- [24] T.N. Taddeucci et al., *Nucl. Phys. A* 469 (1987) 125.
- [25] F. Osterfeld et al., *Phys. Rev. C* 45 (1992) 2854.